Published in "CHIMIA International Journal for Chemistry 72 (4): 249–252, 2018"
which should be cited to refer to this work.

Ag Nanoencapsulation for Antimicrobial Applications

Sarah-Luise Abram§, Jacinthe Gagnon, Magdalena Priebe, Nelly Hérault, and Katharina M. Fromm*

Abstract: Biomaterial-related infections remain a significant challenge in medicine. Antimicrobial materials on the basis of Ag nanoparticles represent a promising solution for this issue. Therefore several Ag-containing nanocontainers and nanorattles have been synthesized and characterized that exhibit remarkable control over the release of Ag^+ as antimicrobial active species. Their biological evaluation against prokaryotic as well as eukaryotic cells reveals that they fulfill the prerequisites for applications as antimicrobial implant coatings.

Keywords: Antimicrobial activity · Implant infections · Nanocontainers · Nanorattles · Silver nanoparticles

Introduction: Ag as Potential Solution to Implant Infections

Silver has been used for its beneficial properties for many years, *e.g.* to preserve drinking water from microbial contamination. Today, the interest in silver as an antimicrobial agent recurs in the context of the increasing resistance of pathogens to the 20th century antibiotics.[1] Multidrug-resistant microbes are surprisingly susceptible to Ag as its antimicrobial action is based on a variety of mechanisms,[2] most of which are related to Ag^+ ions that interact with amino acids or DNA, inhibiting the respiratory chain or blocking the reproduction. Formation of reactive oxygen species and direct damage of the cell membranes are also under discussion.

Metallic silver releases Ag^+ ions from the surface in presence of oxygen. This effect can be enhanced by increasing the ratio of surface to bulk atoms, using Ag nanoparticles (AgNP). AgNP-based antimicrobial coatings should possess thus properties to fight implant related infections as these are often caused by multi-resistant bacteria strains.[3] Such coatings must support the 'race for the surface', hence prevent the bacterial attachment to the implant surface while promoting the integration of the device into healthy tissue.[4] If not, adhering bacterial cells will form biofilms that are difficult to eradicate, and the so infected implant needs to be removed and replaced after the infection has cleared. Medical progress and increasing numbers of implant operations will enhance the significance of this problem.

One challenge in the development of silver-based antimicrobial coatings is the control over the Ag^+ ion release, which should be long-lasting and high enough to maintain a biocidal Ag^+ level to prevent the development of resistance, but low enough to ensure good biocompatibility without adverse effects. Antimicrobial coatings based on Ag^+ coordination compounds[5] developed in the Fromm group have shown excellent potential for the short-term treatment of implant associated infections, *i.e.* for perioperative infections with different staphylococci[6] and in synergistic actions with traditional antibiotics.[7] However, longer-lasting protection against the later possible hematogenous infections remains challenging with these coatings. One way to overcome the issue of fast release kinetics is the use of AgNP where oxidative dissolution is required to fully exhaust their antimicrobial potential. This process depends on the environment (pH, ionic strength, organic groups that interact with Ag^+) and might be further controlled by restricting the access to the AgNP surface. This can be achieved by integration of AgNP into biocompatible nanostructures, *e.g.* nanocontainers (NC) can be loaded or doped with Ag^+ or AgNP (*e.g.* see Fig. 1), porous shells can be grown around AgNP resulting in core-shell particles, or AgNP can be encapsulated inside nanorattles (NR or yolk-shell particles, *e.g.* see Fig. 4).[8] Encapsulation of NP prevents their aggregation/coalescence and preserves their functionality. NC and NR offer additionally a confined space with controlled environment that is advantageous for applications in catalysis as nanoreactors or in drug delivery by providing space for further active compounds, *e.g.* in theranostics.[9] The shell material further offers ways for surface functionalization to enable covalent attachment to biomaterials or inclusion of targeting moieties.

The synthesis of hollow nanostructures such as NC and NR can be roughly divided into three approaches for the void creation:

*Correspondence: Prof. Dr. K. M. Fromm
University of Fribourg, Department of Chemistry
Chemin du Musée 9, CH-1700 Fribourg
E-mail: katharina.fromm@unifr.ch

The first possibility is the use of soft templates such as emulsion droplets, supramolecular micelles, polymeric vesicles or gas bubbles. The second, more widely used way are hard templates, which are first coated with the shell and then removed in a second step by selective dissolution or calcination. These solid materials include polymers, oxides, carbon, metals or ceramics. Besides these two general approaches a third category is proposed for so-called 'self-templating' methods where the material of the 'template' and the shell are either very similar or the same. Surface-protected etching, Ostwald ripening, galvanic replacement or the Kirkendall effect are typically assigned to this group.[10] Others allocate these processes to the hard template methods referring to them as special 'sacrificial' template methods.[11] A synthesis pathway could also combine features of several of these categories (*e.g.* microemulsions and self-templating).[12]

In this context, different types of Ag@porous oxide nanoparticles have been investigated for their potential as antimicrobial implant coatings in correlation with their morphology at the nanoscale by studying their properties in biological environments. This review provides an overview of the Ag nanomaterials developed so far in the Fromm group.

Results and Discussion: Encapsulation of Ag into Hollow Nanospheres

Polystyrene Template Methods: Ag-Ceria and Ag-Titania Nanocontainers

The synthetic routes presented in this section belong to the hard template methods and consist of the coating of anionic polystyrene (PS) spheres with the desired shell materials: ceria and titania (CeO_2 and TiO_2). PS spheres can be synthesized without difficulty in various diameters and are easily removed by either dissolution in *e.g.* toluene,[13] THF,[14] xylene containing trimethylamine[15] or chloroform,[16] or by calcination at a minimum temperature of 500 °C. For the synthesis of silver containing hollow ceria NC ($AgNO_3$-CeO_2 and Ag-CeO_2, Figs 1 and 2, A and B) 220 nm PS spheres were coated with CeO_2 by hydrolysis of $Ce(acac)_3$ in a sol-gel process.[17] The PS template was removed by calcination at 600 °C in order to obtain hollow CeO_2 NC with a diameter of 175–200 nm and with 12–20 nm thick walls. They were soaked in a saturated ethanolic $AgNO_3$ solution, resulting in a loading of 0.77 wt% silver into the $AgNO_3$–CeO_2 NC after three washing steps. Short exposure to daylight caused a partial reduction of the incorporated Ag^+ to AgNP because CeO_2 can be easily photosensitized.

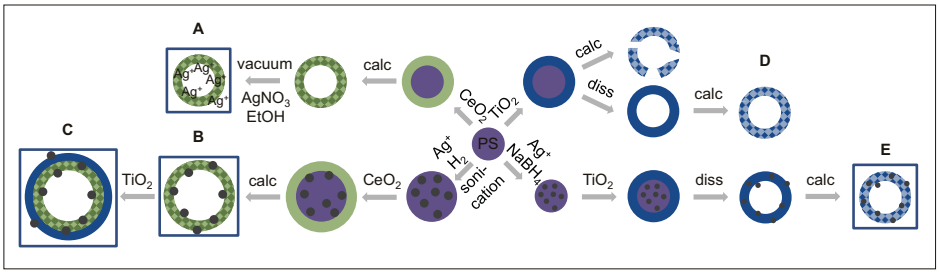

Fig. 1. Synthesis of $AgNO_3$-CeO_2 NC (A), Ag-CeO_2 NC (B), Ag-CeO_2@TiO_2 NC (C), TiO_2 NC (D), and Ag-TiO_2 NC (E) from PS template nanospheres. The frames indicate the NC that were investigated for their antimicrobial properties.

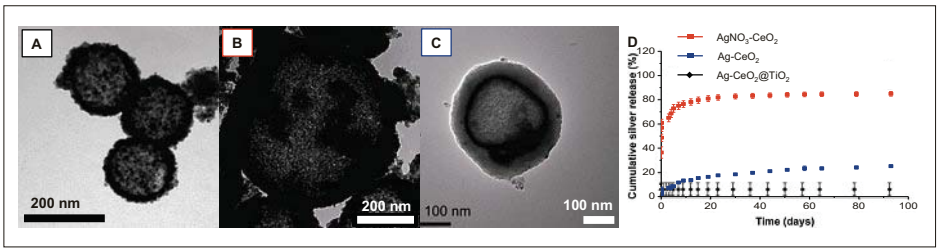

Fig. 2. Transmission electron micrographs of $AgNO_3$-CeO_2 NC (A), Ag-CeO_2 NC (B), Ag-CeO_2@TiO_2 NC (C) and their cumulative Ag^+ release (D), (modified from refs [17] and [18])

As the release of Ag^+ is the key factor for antimicrobial activity it was quantified by inductively coupled plasma optical emission spectroscopy (ICP-OES) of supernatants taken from $AgNO_3$–CeO_2 immersed in water. A fast burst release within 5 days was followed by a 3 week period of slow release (see Fig. 2D). After *ca.* 4 weeks the cumulative Ag^+ release reached a plateau at about 85% of the total Ag content.

To prolong the Ag^+ release, $AgNO_3$ was replaced with AgNP that were synthesized in presence of the PS template beads *via* reduction of $AgNO_3$ with H_2.[17] Coalescence, induced by sonication, embedded the AgNP in the PS spheres, following which these beads were coated with ceria. Calcination resulted in polydisperse Ag-PS@CeO_2 NC (150 nm – 2 µm) with a Ag content of 0.07 wt% and a ceria shell thickness of 15–20 nm (see Fig. 2B). A continuous release profile of Ag^+ in water with less than 30% of the total Ag content set free after three months makes this type of NC a promising candidate for long term infection prevention (Fig. 2D).

To further prolong the Ag^+ release, the Ag-CeO_2 NC were subjected to an additional coating process with titania (Figs 1 and 2, C), resulting in Ag-CeO_2@TiO_2 NC with a 30–60 nm TiO_2 layer.[18] These NC could be subjected to a calcination step in order to transform the amorphous coating into a crystalline one (anatase). For pure CeO_2@TiO_2 NC this procedure increased the pore sizes of the material from 2–5 to 6–8 nm. As the Ag^+ release is expected to be lower with small pores, a higher potential for Ag^+ retention is attributed to amorphous TiO_2 shells. Indeed, already after one day, the Ag^+ ion release from amorphous Ag-CeO_2@TiO_2 in water stagnates after an initial burst corresponding to 7 wt% of the total Ag content (see Fig. 2D), which was attributed to small AgNP that migrated to the surface of the NC during synthesis. After three months of silver retention, the total remaining Ag of the samples was released by addition of concentrated nitric acid. This shows the potential for an on-demand, triggered release of Ag^+ ions from the containers only in presence of bacteria, as many microbial species tend to acidify their environment.[19]

The antimicrobial efficacy was verified for all NC by agar diffusion assays using 90 mg pellets on *E. coli* cultures. They showed a clear antimicrobial effect by visible inhibitions zones around the pellets (Fig. 3). The extent of bacterial inhibition follows the trend of the materials to release Ag^+. Due to the higher release from the $AgNO_3$-CeO_2 NC their inhibition zone was larger (4 mm vs. 2 mm) than for Ag-CeO_2. Despite the exceptional control over the Ag^+ ion release even for Ag-CeO_2@TiO_2 a small inhibition zone could be detected (0.5 mm).

As titania shells demonstrated such efficient control over the Ag^+ ion release the same synthetic approach was used to synthesize pure TiO_2 NC.[16] The emulsion polymerization resulted in 190 nm PS spheres that were coated with TiO_2 by hydrolysis and condensation of titanium isopropoxide similar to the synthetic route of Imhof (Fig. 1D).[13] Several ways to remove the PS core were investigated. The dissolution of PS by liquid–solid extrac-

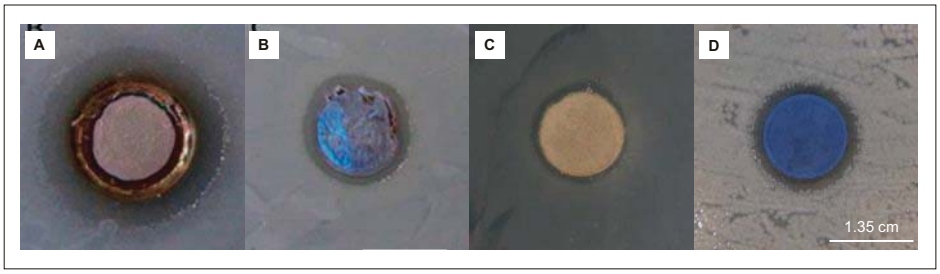

Fig. 3. Antimicrobial activity against *E. coli* by agar diffusion method: $AgNO_3$-CeO_2 NC (A), Ag-CeO_2 NC (B), Ag-CeO_2@TiO_2 NC (C), and Ag-TiO_2 NC (D). (A, B and C modified from refs [17] and [18])

tion with a Soxhlet apparatus and chloroform as solvent was compared to calcination above 500 °C as used for the ceria NC. From 500 °C onward, the PS bands in the IR spectra vanish, while the bands of the O-Ti-O vibration of anatase (400–900 nm)[20] appear. In the case of the Soxhlet extraction of PS, residues remain after the extraction process and had to be removed by an additional calcination step. SEM images showed that if the PS core was removed before calcination the hollow structure could be preserved with intact walls up to a calcination temperature of 500 °C (Fig. 4B). If the core was not removed before thermal treatment, the TiO_2 shells started to break from 300 °C on, as decomposing PS created holes in the shells (Fig. 4A), leaving only debris at 700 °C. At *ca.* 700 °C, destruction occurred regardless of the PS removal pathway and was attributed to ongoing growth of the TiO_2 crystallites as well as the partial crystal phase transition to rutile.

AgNP were thus introduced into homogeneous anatase TiO_2 NC by preforming them on the PS spheres as for the Ag-CeO_2 NC (Fig. 1E), followed by TiO_2 coating, Soxhlet extraction and calcination. The Ag-TiO_2 NC preserved their monodisperse 200 nm diameter with a shell thickness of 20 nm and samples with 6.5 wt% Ag showed an excellent antimicrobial activity against *E. coli* by inducing an inhibition zone of 1.8 mm (Fig. 3D). Gagnon *et al.* have shown a way to attach these types of NC to surfaces *via* sol–gel derived coatings.[21]

Silica-etching Methods: Ag@SiO_2 Nanorattles by Microemulsion and by Surface-protected Etching

Besides the integration of small AgNP into the shells of NC, the nanorattle (NR) setup with a single, moveable core inside a hollow shell was investigated. Here, silica was used as preferred shell material as it easily forms tight silica coatings around preformed metal nanoparticles.[22] Two strategies were exploited to obtain Ag@SiO_2 NR in two different size ranges. The first one is based on a reverse microemulsion synthesis that makes use of the differences in solubility of different silica precursors (Fig. 5A).[12] The reverse microemulsion system is formed by cyclohexane, the surfactant Igepal-CO520 and water or aqueous $AgNO_3$ solutions in the concentration ranges of 0.01–0.2 M. The size of the micelles controls the size of the final nanoparticles. Addition of hydrazine allows first the reduction of Ag^+ inside the water phase to AgNP, while subsequent addition of tetraethyl orthosilicate (TEOS) and (3-aminopropyl)trimethoxysilane (APTMS) results in the formation of silica shells around those AgNP. TEOS tends to be better soluble in the organic, *i.e.* cyclohexane phase, and APTMS, added as ethanolic solution, diffused into the aqueous phase inside the micelles. Thus a silica shell with a structural gradient is formed upon NH_3-induced hydrolysis and condensation. The NR motive is obtained by an etching step of 40 min stirring in warm water (60 °C). The inner part of the silica shell directly around the Ag core is hereby removed preferentially due to its less 'dense' or more 'porous' structure formed from APTMS with one non-hydrolyzable side chain. The resulting 25 nm Ag@SiO_2 NR are presented in Fig. 5A. Depending on the $AgNO_3$ concentration (0.01, 0.05 and 0.1 M) the amount of filled silica containers can be tuned to Ag loadings of 3, 13 and 23 wt%, respectively, as determined by ICP-OES. Higher $AgNO_3$ concentrations during the synthesis result in the formation of large AgNP, loss of the NR structure or even in the formation of uncoated AgNP.

In order to tune the size of the NR void which is limited in the microemulsion approach due to the small size of the micelles, another synthetic approach has been investigated. Ag@SiO_2 core shell particles were transformed into NR by surface-protected etching. Among the countless different synthetic routes to AgNP the polyol process is one of the most studied ones.[23] Ag^+ salts are hereby reduced at elevated temperatures in and by polyols (*e.g.* ethylene glycol) often in presence of surfactants or additional structure directing agents (*e.g.* polyvinylpyrrolidone, PVP). This process was used to synthesize 25 nm AgNP.[24] PVP as capping ligand is known to favor the heterogenic nucleation of silica on metal NP during a sol–gel synthesis over the homogeneous one that would result in pure silica spheres.[22,25] A simple Stöber process[26] could thus be used to obtain homogeneously coated Ag@SiO_2 core shell

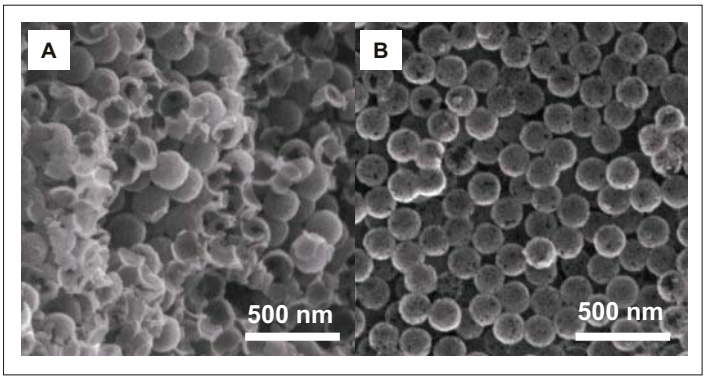

Fig. 4. Scanning electron micrographs of TiO_2 NC (calcination, A) and TiO_2 NC (dissolution + calcination, B) depicting the different level of shell preservation.

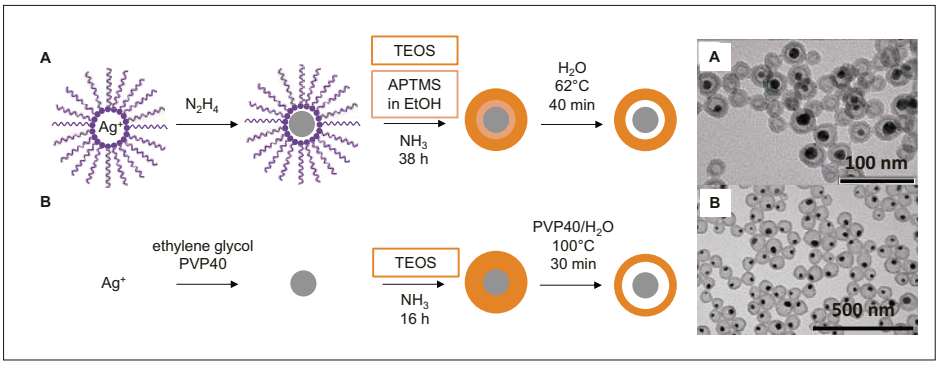

Fig. 5: Synthesis and transmission electron micrographs of Ag@SiO_2 NR by A) microemulsion B) surface protected etching. (A modified from ref. [12]).

particles from the polyol AgNP (Fig. 5B). In an additional etching step in presence of PVP, these core shell particles could be transformed into NR by selective removal of the inner part of the silica shell.[27] PVP is indeed too large to diffuse through the pores of the silica, and hence protects the outer surface of the silica shells from etching.[28] The resulting NR were found in a size range of 80–115 nm in diameter, with a Ag content of about 20–24 wt% (Fig. 5B) and a substantial amount of PVP bound in the system.

Both types of Ag@SiO_2 NR have been evaluated for their antimicrobial efficacy by incubation of different pathogenic Gram-negative and Gram-positive strains in presence of different concentrations of the nanomaterials.[29] The antimicrobial activity is strictly dose dependent in both cases. The surface-protected etching derived NR were compared to their precursor core shell particles. The results will be covered in a future publication.[30] For the smaller, microemulsion-derived NR the Ag content determines the antimicrobial efficacy (Fig. 6). Moreover, an in-depth cytotoxicity evaluation of the smaller microemulsion-derived NR indicates a promising immunotoxicological profile. The *in vitro* experiments show particle uptake by dendritic immune cells in an active phagocytic process without affecting cell viability or inducing inflammation. These types of particles have also been proven to be useful in catalytic degradation studies.[12]

Conclusion and Outlook

A great variety of antimicrobial Ag@ oxide nanoparticles in terms of sizes and composition can be synthesized using three different methods. The choice of synthesis, material, shell thickness, template removal pathway or thermal treatment can all influence the properties, *e.g.* the antimicrobial activity. Ag-CeO_2 and Ag-TiO_2 NC have shown a great potential for prolonging and controlling the Ag^+ release while demonstrating antimicrobial properties, a useful property for implant coatings. Selective dissolution of silica has been exploited for the synthesis of well-defined Ag@SiO_2 NR in two size ranges with potential applicability in catalysis and antimicrobial coatings due to a surprisingly low cytotoxicity. These kinds of evaluations now allow the development of antimicrobial coatings that make use of the tuned Ag^+ release properties ensuring the biological tolerance of the particles.

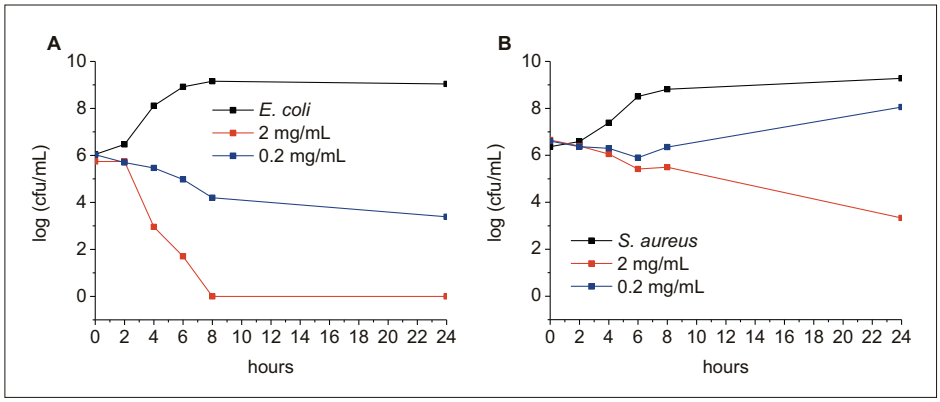

Fig. 6. Representative growth curves of *E. coli* (A) and *S. aureus* (B) in presence of the microemulsion derived Ag@SiO_2 NR containing 23wt% Ag, (modified from ref. [29]).

Acknowledgements

The authors would like to thank the University of Fribourg and the Swiss National Science Foundation, in particular the National Center of Competence in Research "Bio-Inspired Materials" for the generous funding of the project.

Received: January 22, 2018

[1] S. Eckhardt, P. S. Brunetto, J. Gagnon, M. Priebe, B. Giese, K. M. Fromm, *Chem. Rev.* **2013**, *113*, 4708.

[2] H. Zhang, M. Wu, A. Sen, in 'Nano-Antimicrobials: Progress and Prospects', Eds. N. Cioffi, M. Rai, Springer Berlin Heidelberg, Berlin, Heidelberg, **2012**, p. 3.

[3] R. M. Donlan, J. W. Costerton, *Clin. Microbiol. Rev.* **2002**, *15*, 167.

[4] H. J. Busscher, H. C. van der Mei, G. Subbiahdoss, P. C. Jutte, J. J. A. M. van den Dungen, S. A. J. Zaat, M. J. Schultz, D. W. Grainger, *Sci. Transl. Med.* **2012**, *4*, 153rv10.

[5] a) T. V. Slenters, J. L. Sagué, P. S. Brunetto, S. Zuber, A. Fleury, L. Mirolo, A. Y. Robin, M. Meuwly, O. Gordon, R. Landmann, A. U. Daniels, K. M. Fromm, *Materials* **2010**, *3*, 3407; b) T. V. Slenters, I. Hauser-Gerspach, A. U. Daniels, K. M. Fromm, *J. Mater. Chem.* **2008**, *18*, 5359.

[6] R. Kuehl, P. S. Brunetto, A. K. Woischnig, M. Varisco, Z. Rajacic, J. Vosbeck, L. Terracciano, K. M. Fromm, N. Khanna, *Antimicrob. Agents Chemother.* **2016**, *60*, 2467.

[7] M. Varisco, N. Khanna, P. S. Brunetto, K. M. Fromm, *ChemMedChem* **2014**, *9*, 1221.

[8] M. Priebe, K. M. Fromm, *Chem.* **2015**, *21*, 3854.

[9] J. Liu, S. Z. Qiao, J. S. Chen, X. W. Lou, X. Xing, G. Q. Lu, *Chem. Commun.* **2011**, *47*, 12578.

[10] X. Wang, J. Feng, Y. Bai, Q. Zhang, Y. Yin, *Chem. Rev.* **2016**, *116*, 10983.

[11] X. W. Lou, L. A. Archer, Z. Yang, *Adv. Mater.* **2008**, *20*, 3987.

[12] M. Priebe, K. M. Fromm, *Particle & Particle Sys. Charact.* **2014**, *31*, 645.

[13] A. Imhof, *Langmuir* **2001**, *17*, 3579.

[14] A. F. Demirors, A. van Blaaderen, A. Imhof, *Langmuir* **2010**, *26*, 9297.

[15] A.-H. Pei, Z.-W. Shen, G.-S. Yang, *Mater. Lett.* **2007**, *61*, 2757.

[16] N. Hérault, K. M. Fromm, *Helv. Chim. Acta* **2017**, *100*, e1700014.

[17] J. Gagnon, M. J. D. Clift, D. Vanhecke, D. A. Kuhn, P. Weber, A. Petri-Fink, B. Rothen-Rutishauser, K. M. Fromm, *J. Mater. Chem. B* **2015**, *3*, 1760.

[18] J. Gagnon, M. J. D. Clift, D. Vanhecke, I. E. Widnersson, S. L. Abram, A. Petri-Fink, R. A. Caruso, B. Rothen-Rutishauser, K. M. Fromm, *J. Mater. Chem. B* **2016**, *4*, 1166.

[19] L. Zhang, F. Su, X. Kong, F. Lee, K. Day, W. Gao, M. E. Vecera, J. M. Sohr, S. Buizer, Y. Tian, D. R. Meldrum, *RSC Adv.* **2016**, *6*, 46134.

[20] N. Sharotri, D. Sud, *Desalin. Water Treatm.* **2016**, *57*, 8776.

[21] J. Gagnon, R. A. Caruso, K. M. Fromm, *AIMS Bioengin.* **2017**, *4*, 171.

[22] C. Graf, D. L. J. Vossen, A. Imhof, A. van Blaaderen, *Langmuir* **2003**, *19*, 6693.

[23] M. Rycenga, C. M. Cobley, J. Zeng, W. Li, C. H. Moran, Q. Zhang, D. Qin, Y. Xia, *Chem. Rev.* **2011**, *111*, 3669.

[24] P.-Y. Silvert, R. Herrera-Urbina, N. Duvauchelle, V. Vijayakrishnan, K. Tekaia Elhsissen, *J. Mater. Chem.* **1996**, *6*, 573.

[25] K. M. Koczkur, S. Mourdikoudis, L. Polavarapu, S. E. Skrabalak, *Dalton Trans.* **2015**, *44*, 17883.

[26] W. Stöber, A. Fink, E. Bohn, *J. Colloid Interface Sci.* **1968**, *26*, 62.

[27] F. Hu, Y. Zhang, G. Chen, C. Li, Q. Wang, *Small* **2015**, *11*, 985.

[28] Q. Zhang, T. Zhang, J. Ge, Y. Yin, *Nano Lett.* **2008**, *8*, 2867.

[29] M. Priebe, J. Widmer, N. Suhartha Lowa, S. L. Abram, I. Mottas, A. K. Woischnig, P. S. Brunetto, N. Khanna, C. Bourquin, K. M. Fromm, *Nanomed.: Nanotechnol. Biol. Med.* **2017**, *13*, 11.

[30] S. L. Abram, K. M. Fromm, manuscript in preparation, **2018**.